# Correlation functions for the $XY$ model in a Magnetic Field

Wei Zhang [1,2] and H. A. Fertig [1]

[1] *Department of Physics, Indiana University, Bloomington, IN 47405*

[2] *Department of Physics and Astronomy, Ohio University, Athens, OH 45701*

(Dated: February 6, 2008)

## Abstract

Recent studies of the two-dimensional, classical $XY$ magnet in a magnetic field suggest that it has three distinct vortex phases: a linearly confined phase, a logarithmically confined phase, and a free vortex phase. In this work we study spin-spin correlation functions in this model by analytical analysis and numerical simulations to search for signatures of the various phases. In all three phases, the order parameter is nonzero and $< \cos(\theta(\mathbf{r}_1))\cos(\theta(\mathbf{r}_2)) >$ remains nonzero for $r \equiv |\mathbf{r}_1 - \mathbf{r}_2| \to \infty$, indicating the expected long range order. The correlation function for transverse fluctuations of the spins, $C(r) =< \sin(\theta(\mathbf{r}_1))\sin(\theta(\mathbf{r}_2)) >$, falls exponentially in all three phases. A renormalization group analysis suggests that the logarithmically confined phase should have a spatially anisotropic correlation length. In addition, there is a generic anisotropy in the prefactor which is always present. We find that this prefactor anisotropy becomes rather strong in the presence of a magnetic field, masking the effects of any anisotropy in the correlation length in the simulations.

PACS numbers: 64.60.-i, 64.60.Cn, 75.10.Hk

Keywords: correlation function, anisotropy, lattice effects

## I. INTRODUCTION

The two-dimensional classical XY model is important because it serves as a paradigm for many systems, including easy-plane magnets, two dimensional solids, thin film superconductors and superfluids, magnetic bubble arrays, and certain one-dimensional quantum systems. Of particular interest in these systems is the behavior of their topological excitations, which in the $XY$ model are vortices. In spite of the Mermin-Wagner-Hohenberg theorem [1], which forbids long-range order (i.e., a non-vanishing order parameter) at any finite temperature in two dimensions, a (Kosterlitz-Thouless, or KT) phase transition occurs in this system, in which the vortices go from a bound pair phase at low temperature to an unbound vortex phase at high temperature [2]. While the order parameter vanishes in both phases, correlation functions show different behaviors in the different phases. In the high temperature phase, the correlations decrease with increasing distance according to an exponential law [2, 3], while in the low temperature phase, the correlations decrease according to a power law [2, 4].

A non-vanishing order parameter can trivially be restored by the application of a magnetic field which tends to order the $XY$ spins. The behavior of the vortices in this situation [4] has recently been revisited [5, 6, 7] via renormalization group (RG) and simulation studies, leading to the conclusion that vortices can still unbind due to thermal fluctuations in this system, in a two-step process. At the lowest temperatures, vortex-antivortex pairs are linearly confined by a string of overturned spins. As temperature is increased, these strings first undergo a proliferation transition, but the vortices remain confined due to a residual logarithmic attraction. With increasing temperature this attraction is overcome and the vortices deconfine. Importantly, unlike the KT transition, these are not phase transitions in the thermodynamic sense, as they do not lead to singularities in the free energy [5, 6]. Nevertheless, the transitions can introduce singularities in correlation functions [8], and lead to dramatically different behaviors for the physical systems in which the $XY$ model with a magnetic field is realized. This includes the behavior of bilayer thin film superconductors [9], the bilayer quantum Hall system [10], and bosons in a linear optical lattice, tunnel-coupled to a bulk superfluid reservoir [11].

Since a standard way to characterize phases and phase transitions is via the behavior of correlation functions, it is natural to search them for signatures of the deconfinement transitions. In this paper, we study spin-spin correlation functions of the system in all three phases through both analytical analysis and numerical simulations. Due to the external field, all the three phases will have a non-zero order parameter, and for a symmetry-breaking term (i.e., magnetic field coupling) of the form $-h\cos\theta(\mathbf{r})$, with $\theta(\mathbf{r})$ the angular variable of the $XY$ spin located at lattice site $\mathbf{r}$, one easily confirms that the correlation function

$< \cos(\theta(\mathbf{r}_1))\cos(\theta(\mathbf{r}_2)) > \to$ *const.*, for $r = |\mathbf{r}_1 - \mathbf{r}_2| \to \infty$, indicating long range order. A more interesting correlation function $C(r) =< \sin(\theta(\mathbf{r}_1))\sin(\theta(\mathbf{r}_2)) >$ measures the fluctuations of the spins transverse to the direction of the symmetry-breaking field. We find in all three phases $C(r) \sim e^{-r/\lambda}$, but that in the log-confined (Log) phase, $\lambda \equiv \lambda(\alpha)$, with $\alpha$ the angle between $\mathbf{r}$ and the symmetry axis of the underlying lattice. (Throughout this study, we will assume the $XY$ spins reside on a square lattice.) This anisotropy in principle is a signature that distinquishes the Log phase from the linearly confined and deconfined phases. We will see, however, that there is in addition an anisotropy that exists in all three phases (and in the deconfined phase of the $XY$ model without a symmetry-breaking field) which renders the identification of the anisotropy due to the vortex phase very challenging in numerical simulation.

The organization of this article is as follows. In the next section, we study correlation functions in the three phases via some simple analytical models. Section III reports the results of our numerical simulations. Section IV discusses the anisotropy found in our simulations for all the phases, which we show is a ubiquitous effect of the underlying lattice. In Section V we report on attempts to distinquish the lattice anisotropy from that associated with the vortex phase in the numerical data. Conclusions are presented in Section VI.

## II. CORRELATION FUNCTIONS: ANALYTICAL MODELS

The Hamiltonian for the $XY$ model with a magnetic field is

$$H = -K \sum_{<\mathbf{r},\mathbf{r}'>} \cos[\theta(\mathbf{r}) - \theta(\mathbf{r}')] - h \sum_r \cos[\theta(\mathbf{r})], \tag{1}$$

where $< \mathbf{r}, \mathbf{r}' >$ refers to nearest neighbor sites on a two dimensional square lattice. As discussed in the Introduction, we focus on the order parameter and transverse fluctuation correlation functions $< \cos[\theta(\mathbf{r}_1)]\cos[\theta(\mathbf{r}_2)] >$ and $< \sin[\theta(\mathbf{r}_1)]\sin[\theta(\mathbf{r}_2)] >$. Both these can be computed if we can calculate $< e^{i\theta(\mathbf{r}_1) \pm i\theta(\mathbf{r}_2)} >$. A generating functional that allows us to do this is

$$\begin{aligned} Z[J] &=< e^{i\sum_{\mathbf{r}} J(\mathbf{r})\theta(\mathbf{r})} > \\ &\equiv \int D\theta e^{-H + i\sum_{\mathbf{r}} J(\mathbf{r})\theta(\mathbf{r})} / \int D\theta e^{-H}, \end{aligned} \tag{2}$$

where $J(\mathbf{r}) = \delta(\mathbf{r})$ gives the order parameter average, and $J(\mathbf{r}) = \delta(\mathbf{r} - \mathbf{r}_1) \pm \delta(\mathbf{r} - \mathbf{r}_2)$ generates $< e^{i\theta(\mathbf{r}_1) \pm i\theta(\mathbf{r}_2)} >$.

We may study our problem in the Villain model [4, 12, 13]. This essentially involves replacing $e^{J\cos\theta}$ with $\sum_{m=-\infty}^{\infty} e^{-J(\theta - 2\pi m)^2/2}$ wherever it appears in the partition function. The main idea is that the long distance physics depends only on the symmetry of the Hamiltonian, not the details of the interactions.

Following this prescription we may write

$$\begin{aligned} Z[J] &= \sum_{S_{rr'}} \sum_{T_r} \int [D\theta] e^{-\frac{1}{2K}\sum S_{rr'}^2 - \frac{1}{2h}\sum T_r^2} e^{i\sum S_{rr'}[\theta(r)-\theta(r')]+i\sum_r (T(r)+J(r))\theta(r)} \\ &= \sum_{S_{rr'}} \sum_{T_r} \int [D\theta] e^{-\frac{1}{2K}\sum S_{rr'}^2 - \frac{1}{2h}\sum T_r^2} e^{i\sum (\nabla\cdot\mathbf{S}+T+J)\theta(r)}. \end{aligned} \tag{3}$$

Integrating out $\theta$, we have

$$Z[J] = \sum_{S_{rr'}} \sum_{T_r} e^{-\frac{1}{2K}\sum S_{rr'}^2 - \frac{1}{2h}\sum T_r^2} \delta(\nabla \cdot S + T + J). \tag{4}$$

Note that the $\delta$-function appearing here is actually a Kronicker delta with integer arguments. The delta function allows a further simplification if we write

$$\begin{aligned} S_\mu &= \varepsilon_{\mu\nu}\partial_\nu n + A_\mu + \eta_\mu \\ \nabla \cdot \mathbf{A} &= T \\ \nabla \cdot \eta &= J, \end{aligned} \tag{5}$$

where $n$, $\mathbf{A}, \eta$ are integer fields. (Care must be taken in choosing an allowed form of $\mathbf{A}$ such that all configurations of the integer field $\mathbf{S}$ are correctly produced [6].) From Eqs. (4) and (5), we arrive at

$$Z[J] = \sum_{n,\mathbf{A}_\mu} e^{-\frac{1}{2K}\sum |\varepsilon_{\mu\nu}\partial_\nu n + \mathbf{A}_\mu + \eta_\mu|^2 - \frac{1}{2h}\sum |\nabla\cdot\mathbf{A}|^2}. \tag{6}$$

### A. Linearly Confined Phase

In the linearly confined phase, the integerness of $n$ and $A$ is unimportant [6], and we may treat them as continuous fields. Integrating them out, we find the generating functional takes the form

$$Z[J] = e^{-\frac{1}{2K}\int d^2q \frac{|J(q)|^2}{1/\xi^2 + q^2}}, \tag{7}$$

where $\xi = \sqrt{K/h}$. $\xi$ has the interpretation of the width of a string connecting a vortex-anti-vortex pair [5, 6].

• Order parameter

For the order parameter, $J(r) = \delta(r), |J(q)| = 1$, and we get

$$< e^{i\theta} >= \frac{1}{[1 + (\xi/a)]^{\pi/2K}}. \tag{8}$$

• Correlation function

For $< e^{i\theta(\mathbf{r}_1)-i\theta(\mathbf{r}_2)} >$, we take $J(\mathbf{r}) = \delta(\mathbf{r}-\mathbf{r}_1) - \delta(\mathbf{r}-\mathbf{r}_2)$, and using the fact that $< \sin(\theta(\mathbf{r}_1))\cos(\theta(\mathbf{r}_2) >= 0$ by symmetry, we find

$$< \cos(\theta(\mathbf{r}_1))\cos(\theta(\mathbf{r}_2)) - \sin(\theta(\mathbf{r}_1))\sin(\theta(\mathbf{r}_2)) >= e^{-\frac{1}{2K}\int d^2q \frac{1-\cos(qr)}{1/\xi^2+q^2}}, \tag{9}$$

where $r = |\mathbf{r}_1 - \mathbf{r}_2|$.

Similarly, for $< e^{i\theta(\mathbf{r}_1)+i\theta(\mathbf{r}_2)} >$, we take $J(\mathbf{r}) = \delta(\mathbf{r}-\mathbf{r}_1) + \delta(\mathbf{r}-\mathbf{r}_2)$, and find

$$< \cos(\theta(\mathbf{r}_1))\cos(\theta(\mathbf{r}_2)) + \sin(\theta(\mathbf{r}_1))\sin(\theta(\mathbf{r}_2)) >= e^{-\frac{1}{2K}\int d^2q \frac{1+\cos(qr)}{1/\xi^2+q^2}}. \tag{10}$$

Thus we have

$$< \cos(\theta(r_1))\cos(\theta(r_2)) >= \frac{1}{2}[e^{-\frac{1}{2K}\int d^2q \frac{1-\cos(qr)}{1/\xi^2+q^2}} + e^{-\frac{1}{2K}\int d^2q \frac{1+\cos(qr)}{1/\xi^2+q^2}}] \tag{11}$$

and

$$C(r) \equiv < \sin(\theta(r_1))\sin(\theta(r_2)) >= \frac{1}{2}[e^{-\frac{1}{2K}\int d^2q \frac{1-\cos(qr)}{1/\xi^2+q^2}} - e^{-\frac{1}{2K}\int d^2q \frac{1+\cos(qr)}{1/\xi^2+q^2}}]. \tag{12}$$

For large distance r, we have approximately

$$\begin{aligned} &< \cos(\theta(r_1))\cos(\theta(r_2)) >\approx 1 - \frac{1}{2K}\int d^2q \frac{\cos(qr)}{1/\xi^2+q^2} \\ &C(r) \equiv < \sin(\theta(r_1))\sin(\theta(r_2)) >\approx \frac{1}{2K}\int d^2q \frac{\cos(qr)}{1/\xi^2+q^2} \end{aligned} \tag{13}$$

$$C(r) \approx K_0(r/\xi) \sim \sqrt{\frac{r}{\xi}} e^{-r/\xi}, \tag{14}$$

where $K_0$ is the 0-th modified Bessel function, and the last form of $C(r)$ is valid at large distances.

### B. Logarithmically Confined Phase

In this phase, a suitable Hamiltonian for the long distance physics which preserves the underlying lattice symmetry [6] is

$$H = \frac{1}{2K}\int d^2q \{[q_x^2 + K\rho q_y^2]|\phi_1|^2 + [q_y^2 + K\rho q_x^2]|\phi_2|^2 + \xi^2 |q_x q_y(\phi_1+\phi_2)|^2\}, \tag{15}$$

where the $K\rho q_y^2|\phi_1|^2, K\rho q_x^2|\phi_2|^2$ terms are generated by the renormalization group flows of operators that model the integerness of the fields from which the continuous fields $\phi_1, \phi_2$ were derived. The generating function $< e^{i\int J\theta} >$ can be calculated by the path integral

$$Z[J] = \int D\phi_1 D\phi_2 \exp\{-\frac{1}{2K}\int d^2q \{[q_x^2 + K\rho q_y^2]|\phi_1|^2 + [q_y^2 + K\rho q_x^2]|\phi_2|^2 + \xi^2 |q_x q_y(\phi_1+\phi_2) + J|^2\}\}. \tag{16}$$

Integrating out the fields $\phi_1, \phi_2$, we have

$$Z[J] = \exp\left\{ -\frac{\xi^2}{2K} \int d^2q \frac{|J(q)|^2}{1 + \xi^2 q^2 - \xi^2 q^2 \frac{K\rho(q_x^4 + q_y^4 - q_x^2 q_y^2)}{K\rho(q_x^4 + q_y^4) + q_x^2 q_y^2}} \right\}, \tag{17}$$

so that for large $r$,

$$C(\mathbf{r}) \approx \frac{\xi^2}{2K} \int d^2q \frac{\cos(qr)}{1 + \xi^2 q^2 - \xi^2 q^2 \frac{K\rho(q_x^4 + q_y^4 - q_x^2 q_y^2)}{K\rho(q_x^4 + q_y^4) + q_x^2 q_y^2}}. \tag{18}$$

We see that in the Log phase, the mass terms $\propto K\rho$ generated by the renormalization group flows introduce a characteristic anisotropy in the correlation function $C(\mathbf{r})$. If evaluated at large distance, $C(\mathbf{r})$ depends exponentially with distance, but the correlation length is angle-dependent due to the $K\rho$ term.

### C. Free vortex phase

The free vortex phase occurs at high temperature, where the coefficients $K$ and $h$ are small. The simplest way to understand the form of the correlation functions is to return to the orginal $XY$ model and compute the correlations functions perturbatively. The transverse spin fluctuation correlation function is defined as

$$C(\mathbf{r}_1 - \mathbf{r}_2) = < \sin(\theta(r_1)) \sin(\theta(r_2)) > = \int [D\theta] \sin(\theta_1) \sin(\theta_2) e^{K \sum_{<r,r'>} \cos\left[\theta(r) - \theta(r')\right] + h \sum_r \cos\left[\theta(r)\right]}. \tag{19}$$

To second order in $K$ and $h$ we may expand this as

$$\begin{aligned} &< \sin(\theta(\mathbf{r}_1)) \sin(\theta(\mathbf{r}_2)) > = \int [D\theta] \sin(\theta_1) \sin(\theta_2) \\ &\times \prod_{<\mathbf{r},\mathbf{r}'>} \{1 + K cos(\theta(\mathbf{r}) - \theta(\mathbf{r}')) + \frac{K^2}{2} [cos(\theta(\mathbf{r}) - \theta(\mathbf{r}'))]^2\} \prod_{\mathbf{r}} \{1 + h \cos\theta(\mathbf{r}) + \frac{h^2}{2} \cos^2\theta(\mathbf{r})\} \\ &\approx \sum_{P_j} (\frac{K}{2} + \frac{Kh^2}{16})^{|P_j|}, \end{aligned} \tag{20}$$

where $P_j$ refers to self-avoiding paths connecting $\mathbf{r}_1$ and $\mathbf{r}_2$, and $|P_j|$ is the length of the path. The shortest path gives the dominate contribution, so that $C(r) \sim e^{-r/\lambda}$, with correlation length $\lambda = \dfrac{1}{\ln(2/K) - h^2/8}$. This same result can be obtained by approximating the sum over self-avoiding paths as a sum over all random walks, $\sum_{P_j} \to \sum'_{P_j}$. The summation over random walks can be calculated by a generating function method [14]. We first note that $C(\mathbf{r})$ can be written as

$$\begin{aligned} C(\mathbf{r}) &= \sum'_{P_j} x^{|P_j|} \\ &= \sum_N P_N(\mathbf{r}) x^N \end{aligned} \tag{21}$$

where $x = K/2 + Kh^2/16$, $\mathbf{r} = \mathbf{r_2} - \mathbf{r_1} = (m,n)$, $(m,n)$ are the coordinates of $\mathbf{r}$ and $P_N$ is the number of path of $N$ steps. $P_N$ may be conveniently written in terms of the function $f(z_1,z_2) = z_1 + z_1^{-1} + z_2 + z_2^{-1}$, which obeys the identity $(f)^N = \sum_{k,l} c_{k,l}^N z_1^k z_2^l$, where $P_N(\mathbf{r}) = P_N(m,n) = c_{m,n}^N$. Thus we have

$$P_N(\mathbf{r}) = c_{m,n}^N = \frac{1}{(2\pi i)^2} \int dz_1 dz_2 z_1^{m-1} z_2^{n-1} (f(z))^N. \tag{22}$$

Using eq.(21) and eq. (22) and setting $z_1 = e^{iq_x}, z_2 = e^{iq_y}$, we obtain

$$C(\mathbf{r}) \approx \sum_N P_N x^N = \int \frac{dq_x dq_y}{(2\pi)^2} \frac{e^{i\mathbf{q}\cdot\mathbf{r}}}{1 - 2x[\cos(q_x) + \cos(q_y)]}. \tag{23}$$

For small $x$ and large $r$, the integral may be evaluated leading again to the result $C(r) \sim e^{-r/\lambda}$, with $\lambda = \dfrac{1}{\ln(1/x)} = \dfrac{1}{\ln(2/K) - h^2/8}$.

Using similar methods, the order parameter and order parameter correlation function may be shown to behave as

$$\begin{aligned} &< \cos(\theta) > \sim \frac{h}{2}, \\ &< \cos\theta(r_1)\cos\theta(r_2) > \sim \frac{h^2}{4} + e^{-r/\lambda}, \\ &\lambda = \frac{1}{\ln(2/K) - 3h^2/8}. \end{aligned} \tag{24}$$

Finally, we note that similar results may be obtained within the Villain model, although the derivation is considerably more involved than this.

## III. NUMERICAL SIMULATION

In the previous section, we found a characteristic anisotropy in the Log phase that is not present in either the linearly confined or unbound vortex phases by computing correlation functions near fixed points of these phases [5, 6]. We now search for this behavior in simulations. We shall see that anisotropy in the correlation functions is quite generic in the $XY$ model, presumably due to irrelevant operators that were not included in our effective Hamiltonians. Our results suggest that very high precision simulations are needed to detect the effects of the vortex phase in the correlation functions.

We employ a standard Langevin dynamics approach for our simulations. Angular variables $0 \leq \theta < 2\pi$ are represented on a square lattice with periodic boundary conditions. The model is equivalent to that of an array of superconducting grains, treated within the resistively shunted Josephson junction model [15]. The equations of motion for the angular variables are

$$\Gamma \frac{d^2\theta(\mathbf{r})}{dt^2} = \frac{\delta H_{XY}}{\delta\theta(\mathbf{r})} + \zeta(\mathbf{r}) - \eta \frac{d\theta(\mathbf{r})}{dt}. \tag{25}$$

The spin stiffness was taken as $K = 1$, setting our unit of energy. The effective moment of inertial for the spins $\Gamma$ were also taken to be 1, setting the unit of time in our simulation. The viscosity $\eta$ was taken to be 0.1, which we found yields good equilibration times and statistics. $\zeta(\mathbf{r}, \mathbf{t})$ is a random torque satisfying $< \zeta(\mathbf{r}, t)\zeta(\mathbf{r}', t') >= 2\eta T \delta_{\mathbf{r},\mathbf{r}'}\delta(t - t')$ with $T$ being the temperature of the system (chosen to be 1.2 for the results discussed below.) The system size is $N_x = N_y = 61$. Our Hamiltonian $H_{XY}$ takes the form

$$H_{XY} = -K \sum_{<\mathbf{r},\mathbf{r}'>} cos[\theta(\mathbf{r}) - \theta(\mathbf{r}')] - h \sum_{\mathbf{r}} cos[\theta(\mathbf{r})], \tag{26}$$

with $K = 1$. A typical run consists of $5 \times 10^7$ time steps. Each time step is 0.1 (in units of $\sqrt{\Gamma/K}$). We also eliminated the initial $2 \times 10^6$ steps in these runs for equilibration. We repeated runs for each set of parameters with several different seeds, allowing us to estimate the statistical error.

Our simulation results are summarized in Fig. 1-4. The curve with solid dots (squares) is for the transverse spin fluctuation correlation function $C(\mathbf{r})$ in the $x$ ($y$) direction. Stars show correlation functions along a direction with angle $\pi/4$ with respect to the $x$ axis. Fig. 1 shows results for $h$=0, while Figs. 2, 3 and 4 are respectively for $h = 0.417, 0.25$ and 0.15. These values were chosen to place the system in the linearly confined, Log, and unbound vortex phase, respectively, as found in an earlier study in which the vortex phase was probed by measuring fluctuations in the vortex dipole moment of the system [7].

In all the simulations, we see clearly that $C(r) \sim e^{-r/\lambda}, r = |\mathbf{r}_1 - \mathbf{r}_2|$; i.e., the correlation function falls exponentially at large distances. This agrees with our expectations from Section II. The correlation functions in the $x$ and $y$ directions are the same within the numerical accuracy of the simulations, as expected from the lattice symmetry. There is also a small difference between the amplitudes of the correlation functions along the bond direction and along the diagonal. However, the form of this anisotropy is *not* what we expect from Section II, which suggested anisotropy in the correlation length in the Log phase. This should lead to different slopes for $C(r)$ in the log-log plots along the bonds and the diagonals at large distances. Although there is some evidence for this, it occurs only at very large distances, where our statistics are relatively poor and an accurate measurement was not possible.

That most of the anisotropy appears as an offset in the correlation functions in the log-log plots suggests that our results are dominated by the prefactor of the exponential function for $C(r)$. We explain the origin of this in the next section, and argue that it is a generic behavior that is independent of the vortex phase of the system.

## IV. LATTICE EFFECTS

To take the lattice effects into account, the integration in eq. (7)

$$\int d^2q \frac{|J(q)|^2}{1/\xi^2 + q^2} \tag{27}$$

should be modified to

$$\int d^2q \frac{|J(q)|^2}{1/\xi^2 + 4 - 2cos(q_x) - 2cos(q_y)} \tag{28}$$

where our unit of length is the bond length. Following the methods of Section II, the resulting transverse spin fluctuation correlation function becomes

$$C(r) \sim \int d^2q \frac{\cos qr}{1/\xi^2 + 4 - 2cos(q_x) - 2cos(q_y)}. \tag{29}$$

For large distances, $C(r)$ may be calculated using the stationary phase approximation [16, 17], with the result

$$C(r) = \frac{exp[-q_x^* m_x - q_y^* m_y]}{(|m|/R)^{1/2}}. \tag{30}$$

Here $\mathbf{r} = (m_x, m_y)$, and $q_x^*, q_y^*$ are determined by

$$\begin{aligned} 1/\xi^2 &= 4 - 2\cosh(q_x^*) - 2\cosh(q_y^*) \\ m_y \sinh(q_x^*) &= m_x \sinh(q_y^*), \end{aligned} \tag{31}$$

and $R$ is given by

$$R = \frac{\sqrt{\sinh^2(q_x^*) + \sinh^2(q_y^*))}}{|\sinh^2(q_x^*)\cosh(q_y^*) + \sinh^2(q_y^*)\cosh(q_x^*)|}. \tag{32}$$

For large $\xi$, the solution to Eq. 31 is

$$\begin{aligned} q_x &= \frac{1}{\xi}\cos\alpha \\ q_y &= \frac{1}{\xi}\sin\alpha, \end{aligned} \tag{33}$$

where $\tan\alpha = m_y/m_x$. In this case, the correlation length is $\lambda = \xi$ and

$$R = \frac{\xi}{1 + (a/\xi)^2 \sin^2(\alpha)\cos^2(\alpha)}. \tag{34}$$

Thus we see that the lattice structure induces anisotropy in the prefactor of the correlation function. The ratio of the correlation function along two different directions, with angles $\alpha_1, \alpha_2$ with respect to the $x$ axis, has the form

$$\frac{C(r,\alpha_1)}{C(r,\alpha_2)} = \sqrt{\frac{R(\alpha_1)}{R(\alpha_2)}} = 1 + \frac{1}{8}(\frac{a}{\xi})^2(\sin^2(2\alpha_2) - \sin^2(2\alpha_1)) \tag{35}$$

TABLE I: Fitting parameter I

| $h$ | $A$ | $\xi$ | $K\rho$ | $a$ | $b$ |
|---|---|---|---|---|---|
| 0.0 | 0.5165 | 4.6173 | -0.1940 | -0.8616 | 0.3821 |
| 0.25 | 0.08154 | 1.7834 | -0.03805 | -0.1673 | 0.3765 |
| 0.417 | 0.05268 | 1.4154 | -0.007307 | -0.1095 | 0.3060 |

for $a/\xi << 1$. This prefactor anisotropy persists even at very long distance, and shows up as an offset in a plot of $C(r)$ along different directions when displayed in a log-log plot. This is exactly what we see in our numerical simulation, and it is apparent that for the distances where we can make reliable measurements, it is the dominent effect. We note that, although this result was presented for the linearly confined phase, one may show that in all the phases discussed in Section II, a lattice regularization of the momentum integrals leads to similar effects.

## V. DISCUSSION

As discussed above, there is anisotropy in the correlation functions for all three phases due to lattice regularization. One can search for extra anisotropic behavior in the Log phase, as in the section II. To separate the two kinds of anisotropies, we fit our numerical results by the formula

$$C(r) = A \int d^2q \frac{\cos(qr)}{1 + \xi^2 q^2 - \frac{K\rho q_x^2 q_y^2}{q^2} + aq^4 + bq_x^4 q_y^4}. \tag{36}$$

We choose the general form $\frac{K\rho q_x^2 q_y^2}{q^2}$ (compatible with lattice symmetry) to mimic the anisotropic behavior apart that should not arise due to the lattice effects but is expected in the Log phase. The term $aq^4$ is a higher order isotropic term and the term $bq_x^2 q_y^2$ is the anisotropic term due to lattice effects, expected from expanding the cosines in a lattice regularization, and which for large enough distances should be the leading order corrections due to this regularization. We fit our numerical curves for the correlation function within a suitable distance interval (generally from 3 to 6 correlation lengths.) If the distance is too small, short distance correlations become important and presumably need further terms to be correctly modeled. On the other hand, when $r$ is too large, $C(r)$ becomes very small, and numerical errors spoil the fit. The resulting fitting parameters are shown in Table I.

We see that $K\rho$ is small but nonzero for all three phases, and moreover is largest when $h = 0$ when we expect no such term. We believe this is due to the fact that one needs to

TABLE II: Fitting parameter II

| $h$ | $A$ | $\xi$ | $a$ | $b$ |
|---|---|---|---|---|
| 0.0 | 0.5163 | 4.6207 | -1.1499 | 3.0605 |
| 0.25 | 0.08097 | 1.7884 | -0.1800 | 0.5610 |
| 0.417 | 0.05256 | 1.4167 | -0.1110 | 0.3311 |

measure the correlation function at much larger distances than we can achieve numerically to see its true asymptotic behavior. This is consistent with earlier simulations [7] which required detection of vortex-antivortex pairs at effective separations of order the system size, typically $\sim$5 times larger than the maximum $r$ used in our fits. To support this point of view, we fitted our numerical results by Eq. 36, but set $K\rho = 0$ by hand; i.e.,

$$C(r) = A \int d^2q \frac{\cos(qr)}{1 + \xi^2 q^2 + aq^4 + bq_x^4 q_y^4}. \tag{37}$$

The obtained fitting parameters are listed in Table II.

To further compare the fits with one another and the numerical data, we use Eqs. 36 and 37 to calculate model correlation functions over long distances with the fit parameters. The difference between these turns out to be extremely small even at large distances. (For $h = 0.0$, it is 0.81%; for $h$=0.25, it is 4.9%; for $h$=0.417, it is 4.0%.) The absolute difference is $3.3\times10^{-4}$ for $h$ =0.0; $2.8\times10^{-5}$ for $h$=0.25; and $4.9\times10^{-6}$ for $h$=0.417. Most importantly, in all cases these differences are of the same order or smaller than our numerical error. To demonstrate this, in Fig. 5 we compare the correlation functions $C(r)$ (both along a bond direction and along the diagonal) for $h$=0.25, obtained by numerical simulation, from Eq. 36, and from Eq. 37. The curves from the three methods are nearly indistinquishable. In the inset, we show the correlation function for an arbitrary direction, $\tan(\alpha) = 1/2$, where $\alpha$ is the angle with respect to the $\hat{x}$ axis. Again, we can hardly see any difference among the curves. Clearly, much higher precision data than we were able to generate is required to distinquish the effects of lattice anisotropy from the effects of logarithmically bound vortices.

## VI. CONCLUSION

We have discussed the effect of the various vortex phases of the $XY$ model in a magnetic field on spin correlation functions, focusing on transverse spin fluctuations. Calculations based on the fixed point Hamiltonians suggest that the Log phase should have a unique signature in an anisotropic correlation length, but there is anisotropy common to all the phases due the lattice realization of the model, that shows up as irrelevant operators in the

renormalization group. Distinquishing these lattice effects from those of the vortex phase turns out to be quite difficult for system sizes and run times that are readily attainable in our Langevin dynamics simulations. While we believe the anisotropy is present, direct confirmation will require higher accuracies and larger systems than were achieved in our own study.

**Acknowledgments** This work was supported by the NSF through Grant Nos. DMR-0454699 and DMR-0511777.

---

[1] N. D. Mermin and H. Wagner, Phys. Rev. Lett. 17, 1133 (1966). P. C. Hohenberg, Phys. Rev. 158, 383 (1967).

[2] J. M. Kosterlitz, D. Thouless, J. Phys. C 6, 1181 (1973); J. M. Kosterlitz, J.Phys. C 7, 1046 (1974).

[3] R. A. Pelcovits, J. Phys. A: Math. Gen. 14, 1693 (1981).

[4] J. V. José, L. P. Kadanoff, S. Kirkpatrick, and D. R. Nelson, Phys. Rev. B **16**, 1217 (1977).

[5] H. A. Fertig, Phys. Rev. Lett. 89, 035703 (2002).

[6] H. A. Fertig and Kingshuk Majumdar, Ann. Phys. 305, 190 (2003).

[7] H. A. Fertig and Joseph P. Straley, Phys. Rev. B. **66**, 201402(R) (2002).

[8] D. Ruelle, Statistical Mechanics: Rigorous Results, Addison-Wesley, Reading, MA, 1989.

[9] Wei Zhang, H. A. Fertig, Phys. Rev. B. **71**, 224514 (2005).

[10] S. M. Girvin and A. H. MacDonald, *Multicomponent Quantum Hall Systems: The Sum of Their Parts and More*, in Perspectives in Quantum Hall Effects, edited by S. Das Sarma and A. Pinczuk, (Wiley, New York, 1997).

[11] K. Majumdar and H. A. Fertig, Phys. Rev. Lett. **94**, 220402 (2005)

[12] J. Villain, J. Phys. **36**, 581 (1975).

[13] L. P. Kadanoff, *Statistical Physics: Dynamics, Statics, and Renormalization* (World Scientific, Singapore, 2000).

[14] E. W. Montroll, and G. H. Weiss, J. Math. Phys. 6, 167 (1965).

[15] M. V. Simkin and J. M. Kosterlitz, Phys. Rev. B 55, 11646 (1997).

[16] E. N. Economou, Green's functions in quantum physics, (Springer-Verlag, Berlin; New York, 1983).

[17] J. Callaway, J. Math. Phys. 5, 783 (1964)

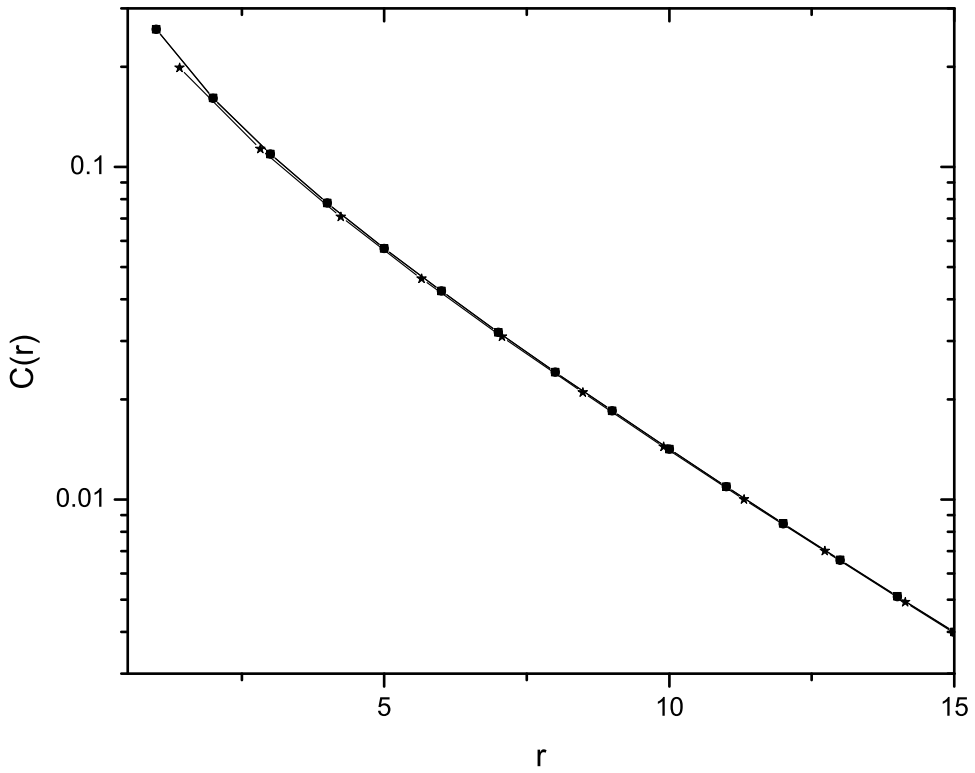


FIG. 1: Correlation functions vs. distance in a log-linear plot for $h$=0, system size=61. Averaged over 9 seeds. Curves with solid dots and squares are for correlation functions in the $x$ and $y$ directions, and cannot be distinquised in the figure, indicating the errors are smaller than the symbol sizes. Curve with stars is for correlation function in the direction with angle $\pi/4$ with respec to $x$ axis.

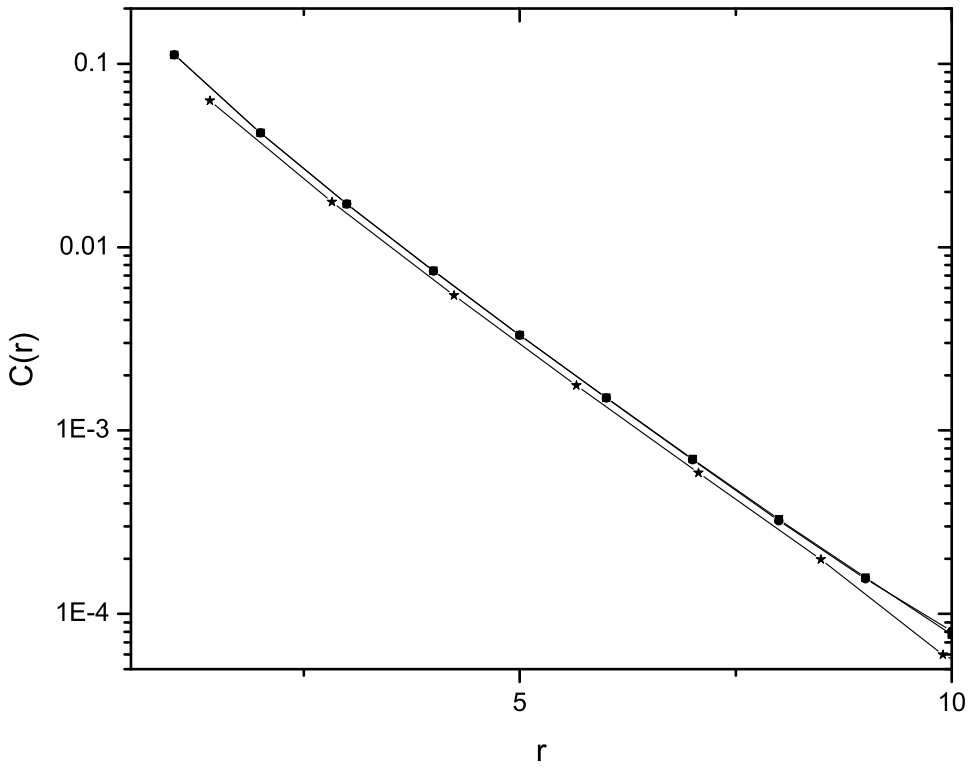


FIG. 2: Correlation functions vs. distance in a log-linear plot. $h$=0.417 (linearly confined phase), system size=61. Averaged over 7 seeds. Curves with solid dots and squares are for correlation functions in the $x$ and $y$ directions, and cannot be distinquised in the figure, indicating the errors are smaller than the symbol sizes. Curve with stars is for correlation function in the direction with angle $\pi/4$ with respec to $x$ axis.

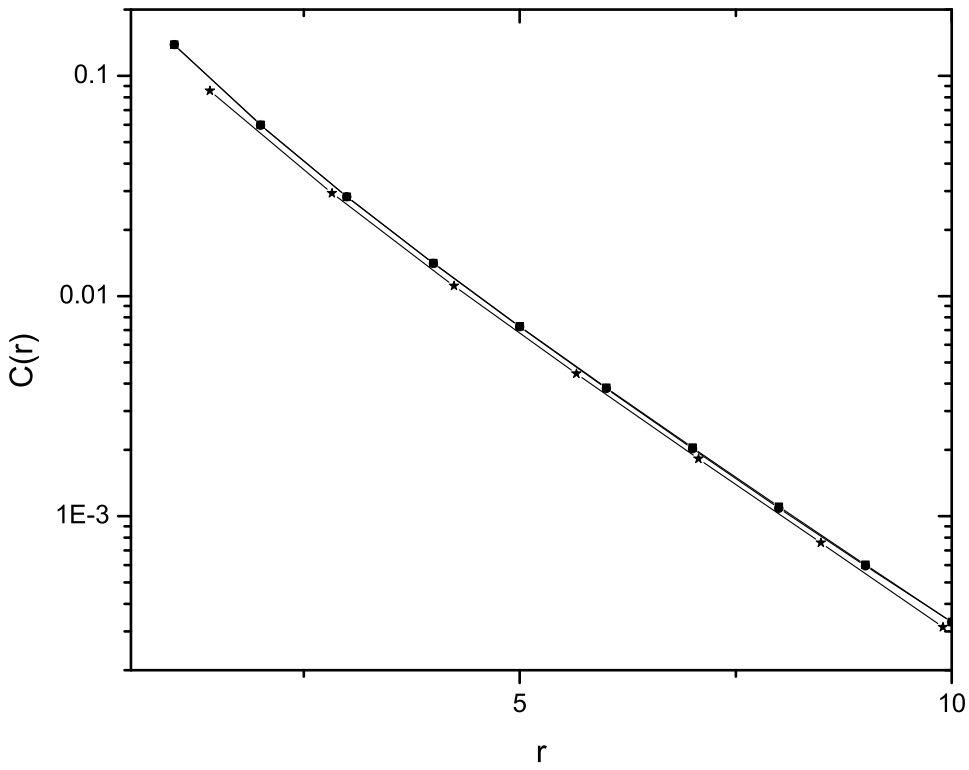


FIG. 3: Same as Fig. 2, except $h$=0.25 (Log confined phase), and data is averaged over 5 seeds.

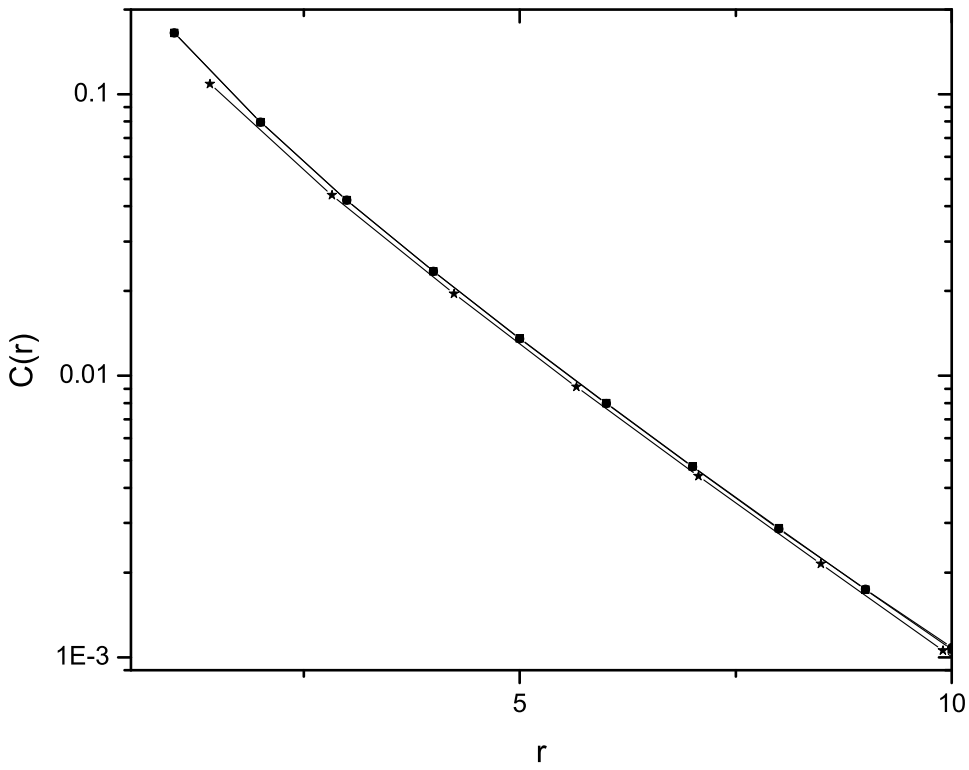


FIG. 4: Same as Fig. 2, except $h$=0.15 (free vortex phase), and data is averaged over 2 seeds.

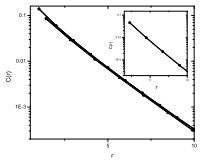

FIG. 5: Correlation functions vs. distance in a log-linear plot. $h$ =0.25 (Log confined phase), system size=61. The two linesin the main panel (for $x$ direction and the direction with angle $\pi/4$ with respect to $x$ axis are actually two pairs of three overlapping curves: the results obtained from numerical simulation, fitting formula Eq. 36 and fitting formula Eq. 37, demonstrating that our data do not distinquish the expected anisotropy in the Log phase from lattice anisotropy effects. In the insert are correlation functions in the direction with angle $\tan\alpha = 1/2$. Two curves obtained from Eqs. 36 and 37 are again indistinquishable.